May 17th, 2:50 PM

Numerical and Physical Study on the Energy Dissipation at Inflatable Gates

Michael Gebhardt
Bundesanstalt für Wasserbau, michael.gebhardt@baw.de

Udo Pfrommer
Bundesanstalt für Wasserbau, udo.pfrommer@baw.de

Tobias Rudolph
Wacker Ingenieure

Carsten Thorenz
Bundesanstalt für Wasserbau, carsten.thorenz@baw.de

Recommended Citation

Gebhardt, Michael (2018). Numerical and Physical Study on the Energy Dissipation at Inflatable Gates. Daniel Bung, Blake Tullis, 7th IAHR International Symposium on Hydraulic Structures, Aachen, Germany, 15-18 May. doi: 10.15142/T3JD26 (978-0-692-13277-7).

7th International Symposium on Hydraulic Structures Aachen, Germany, 15-18 May 2018
ISBN: 978-0-692-13277-7 DOI: 10.15142/T3JD26

Numerical and Physical Study on the Energy Dissipation at Inflatable Gates

M. Gebhardt[1], U. Pfrommer[1], T. Rudolph[2] & C. Thorenz[1]
[1] *Federal Waterways Engineering and Research Institute (BAW), Karlsruhe, Germany*
[2] *Wacker Ingenieure, Birkenfeld, Germany*
E-mail: michael.gebhardt@baw.de

Abstract: *Inflatable gates have a number of advantages when compared with standard steel gates. In case of flood the rubber membrane is deflated to a flat structure and placed on the weir sill. This paper deals with the energy dissipation at inflated gates, in particular the influence of the weir sill on the design of the stilling basin with respect to the described boundary conditions. Numerical investigations were carried out using OpenFOAM (Open source Field Operation and Manipulation). Additionally, experiments were performed in a physical model. The hydraulic characteristic of low Froude hydraulic jumps, turbulent flow structures, and the energy dissipation mechanisms during overflow are presented and discussed.*

Keywords: *Inflatable gate, weir, energy dissipation, stilling basin, hydraulic jump, low Froude number*

1. Introduction

An inflatable rubber gate consists of a multi-ply rubber membrane, which is fixed to the weir sill using clamp plates and anchor bolts. The gate is inflated by pumping air or water inside the rubber body until the design height or design pressure is reached. It is deflated by allowing the air or water inside the rubber body to escape. The simplicity and flexibility of the structure is a key consideration in its wide scope of applications. With an appropriate design, the height of the weir sill can reach 25-30% of the upstream flow depth without a “noticeable” backwater effect, which is advantageous not only for costs but also for maintenance (Gebhardt et al. 2012). The weir sill of a rubber gate is characterized by a broad horizontal crest where the length is determined by the deflated rubber membrane. In general, the minimum length of the weir sill corresponds to the length of the deflated membrane. In practice the sills are even longer to provide space in order to ease installation and maintenance or to set stop logs. The length of the deflated membrane depends also on the filling medium: The circumference length of an air-filled type is shorter than the water-filled type. Hence, the length of the weir sill can be shorter (PIANC 2018). A comparison is given by JIID (1986) to give the reader an idea of the different sill lengths for an air-filled and for a water-filled type with the same gate height h_d, where h_d is defined as the vertical distance between weir sill and gate crest (Figure 2). The length of a deflated membrane is 1.74 h_d for the air-filled and 2.35 h_d for the water-filled type. Fig. 1 shows different types of weir sills at rubber gates.

Figure 1. Weir sills at rubber gates: Marklendorf, Germany (left) and Ebenhofen, Germany (right).

In low head hydraulic structures, such as inflatable gates, energy dissipation under a low Froude number hydraulic jump is a common hydraulic problem. Poor energy dissipation is leading to large waves in downstream river beds, and erosion might occur. This paper deals with the problem of energy dissipation of inflatable gates and the optimization of the geometry of the weir sill and the stilling basin with respect to the described boundary conditions. The objective of the study was to define a standard stilling basin in order to reduce the necessity for further investigations. Therefore, numerical investigations were carried out using OpenFOAM (Open source Field Operation and Manipulation). The final geometry was tested in an existing physical model.

2. Designing Stilling Basins

2.1. Direct Hydraulic Jump

Stilling basins are used to dissipate the energy of water in order to prevent scouring caused by high velocities downstream of the weir. This scouring might damage the foundation of the dam. The primary method for dissipating energy is to generate a hydraulic jump. Several books discuss a range of design techniques for stilling basins such as Rouse (1967), Chow (1959), or, most recently, Chanson (2009). The design is based on the Froude Number of the approaching flow, which is determined by the head and the geometry of the substructure. If a rubber gate is installed on top of a weir sill, additional energy dissipation takes place on the sill as long as the nappe touches the sill. One of the main objectives of this study was to develop a standard which could be used in the future and minimize the need for individual model tests.

Today, extensive literature can be found on hydraulic jumps which are reviewed, for instance, in Singh and Hager (1992). More recently, Chanson and Montes (1995) focus on undular hydraulic jumps, which are characterized by a smooth rise of the free-surface followed by a train of well-formed stationary waves. For a rectangular horizontal channel the equation of Bélanger (1941) is used to calculate the conjugate water depth y_2 as a function of the inflow Froude number Fr_1 and the water depth y_1. In Eq. (1) bed friction is neglected.

$$y_2 = \frac{y_1}{2}\left(\sqrt{1 + 8\,Fr_1^2} - 1\right) \tag{1}$$

Applying the energy equation, the energy-head loss ΔH_L due to the violent turbulent mixing and dissipation in the hydraulic jump can be derived:

$$\Delta H_L = H_1 - H_2 = \frac{(y_2 - y_1)^3}{4 y_1 y_2} \tag{2}$$

The ratio $\Delta H_L/H_1$ is known as the relative energy-head loss. Fig. 2 shows a definition sketch.

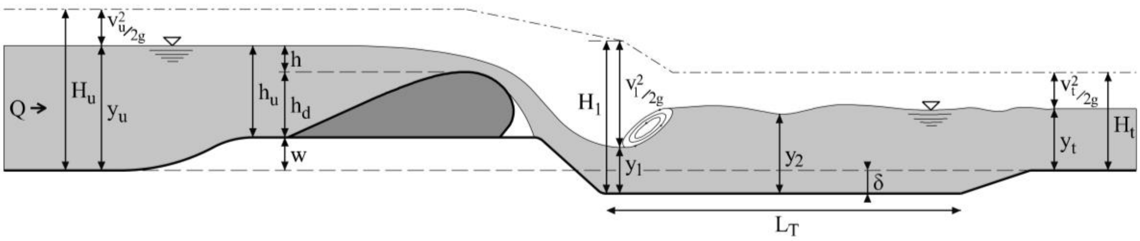

Figure 2. Flow above a rubber gate, definition sketch.

2.2. Hydraulic Jump Classification

In general, the higher the inflow Froude number at the entrance to a basin, the more efficient the hydraulic jump. Typically, the hydraulic jump is classified in dependence of the inflow Froude number. Undular ($Fr_1 < 1.7$), weak ($1.7 < Fr_1 < 2.5$), oscillating ($2.5 < Fr_1 < 4.5$), steady ($4.5 < Fr_1 < 9.0$), and strong jump ($Fr_1 = 9.0$) are the "classical" forms of hydraulic jumps (Chow 1959). Note the formations of these jumps also require an adequate downstream water level. A tailwater depth lower than the conjugate water depth y_2 will lead to supercritical conditions and a tailwater depth higher than the conjugate water depth y_2 to a drowned or submerged hydraulic jump.

In practical problems, the tailwater fluctuates, owing to changes in discharge. Hence, the tailwater rating curve has to be compared with the jump rating curve. If the tailwater depth increases, the jump will be forced upstream, drowned, and will finally become a submerged jump. Against this background the guideline for river bottom protection structures, drop structures, chutes, cascades, and sills (DIN 19661-2 2000) enlarges the above mentioned classification. Undular flow (Type a) occurs when the head is too small to create super-critical conditions below the drop and submerged hydraulic jump (Type b) or partly submerged jump (Type c), where the outflow Froude number is $Fr_2 < 0.5$. Finally, the non-submerged hydraulic jump is introduced for $Fr_2 > 0.5$ (Type d). In order to ensure a high energy dissipation, there exist some recommendations for the submergence ratio ε, which is defined as the ratio of the tailwater depth y_t and the conjugated water depth y_2 with respect to the level of the stilling basin. Hence, the submergence ratio has to be supplemented by the stilling basin depth.

$$\varepsilon = \frac{y_t + e}{y_2} \tag{3}$$

Alternatively, the definition of Rajaratnam (1965) is common for $S_f = (y_t - y_2)/y_2$. According to Blind (1987) the submergence ratio should be in the range $1.05 < \varepsilon < 1.25$. With increasing submergence ratio the energy dissipation will get worse again. This recommendation can also be found in DIN 19661-2 (2000) for drop structures. According to George (1978) or Bollrich *et al.* (2013), the water depths in the basin should be about 5% greater than the computed conjugate depth.

2.3. Length of Hydraulic Jump

The length of the jump cannot be determined easily by theory or in a scale model. It has been investigated by many researchers and quite a number of empirical relations are available (Table 1).

Table 1. Empirical equations for the jump length given by some authors.

Author	Length of hydraulic jump L_T
Woycicki (1931) discussed in Bollrich *et al.* (2013)	$\frac{L_T}{y_1} = 0.05 \left(81\sqrt{1 + 8 \cdot Fr_1^2} - 2 \cdot Fr_1^2 - 241\right)$
Peterka (1984)	$\frac{L_T}{y_1} = k \cdot y_2$ with k = 4.8/5.8/… for Fr_1 = 2.4/4/…
Blind (1987)	$L_T = 4.5 \div 6.0\,(y_2 - y_1)$

2.4. Design Considerations

The design of a stilling basin is a typical question in hydraulic engineering and, most of the time, an individual investigation for one site with its specific boundary conditions. Where standards are available, such as with the United States Bureau of Reclamation (USBR) stilling basins (Peterka 1984) or the St. Anthony Falls (SAF) stilling basin (Blaisdell 1959), the basin type can be chosen according to the inflow Froude number Fr_1, and the dimensions can be determined as a function of the inflow water depth. In general, a stilling basin is designed to dissipate the kinetic energy of the flow in a hydraulic jump, and the objective of the designer is to ensure that the jump is not swept out of the stilling basin. The design involves the determination of the depth, length, and shape of the basin for a design flood, which can be significantly different and lower compared to the design flood of the dam.

Generally, the form of a stilling basin can range from a simple concrete apron to a complex structure including chute blocks, baffles, or end-sills, depending on the inflow Froude Number. Chute blocks, baffles, and end sills are measures to increase the energy dissipation rate and reduce the length. But, today the fish passage through stilling basins is also considered to be a direct cause of injury or mortality or an indirect cause (increased susceptibility of disorientated or shocked fish to predation). Biologists discern the physical impact against energy dissipators as one possible cause for fish damages (Marmulla 2001). Therefore, a conventional stilling basin is considered in this study. However, there are other factors, such as shearing effects, abrasion against surfaces, turbulence, or sudden variations in velocity and pressure. But, they cannot be prevented due to the characteristics of the hydraulic jump phenomenon to develop large-scale turbulence, surface waves, energy dissipation, and air entrainment.

3. Numerical and Experimental Set-Up

The numerical simulations were performed with the open source CFD toolbox OpenFOAM® with the two-phase transient solver interFoam in version 1.6. A detailed description can be found in Rusche (2002). A 3D model with a clear width of 2.11 m was created and discretized with a hexahedral dominant mesh with a base mesh size of 20 cm. Areas where small-scale phenomena like flow detachment occur (e.g., the crest) were discretized up to a mesh size of 2.5 cm (Fig. 3). For turbulence modelling a Large Eddy Simulation (LES) was used which requires a dense grid. Based on preliminary studies the chosen mesh cell size was considered to be sufficient to resolve the large-scale turbulence in a hydraulic jump directly. As computing resources were not a limiting factor for this investigation, it was considered to be advantageous not to use a possibly error-prone turbulence model based on Reynolds-averaging. Three-dimensional transient calculations with stationary boundary conditions were conducted until a quasi-stationary state was achieved. A constant discharge and a variable water level were specified as boundary conditions for the inflow. At the outflow a fixed downstream water level and variable discharge were prescribed. For this, a set of in-house developed boundary conditions was used (Thorenz and Strybny 2012). The cross section of the rubber gate was measured in a physical model and used as geometry for the numerical simulations.

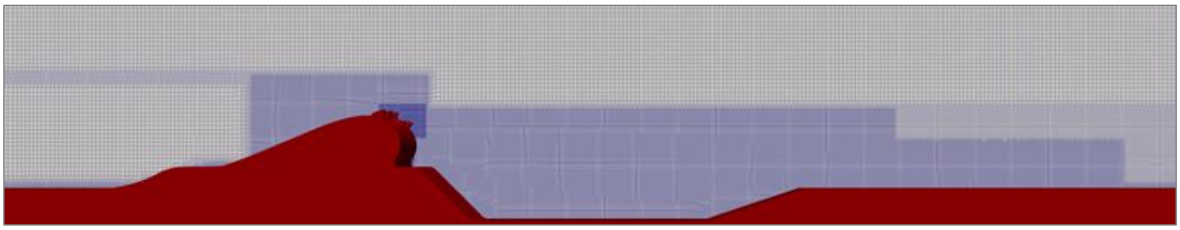

Figure 3. Example of a generated mesh for a partly deflated rubber gate, weir sill and stilling basin - base mesh size of 20 cm, refinement up to 10 cm (air-fluid interface), 5 cm (stilling basin) and 2.5 cm (separation zone at rubber gate).

It should be noted that an accurate prediction of air entrainment is still challenging in numerical models, especially at the free-surface. It was assumed that the high resolution of the LES approach helps to reproduce these effects. In Open FOAM the Volume-of-Fluid (VOF) model is used to capture the interface between two fluids, where the value α defines the ratio of air and water in one cell. For simplicity it is common practice that the interface is represented in post-processing by an isosurface for $\alpha = 0.5$. Against this background it is obvious that air entry into the water simulated by VOF model is different with the prototype experiment but also with the physical model. Physical models are affected by scale effects, with Weber and Reynolds numbers usually being too low to adequately reproduce observed flows.

In order to test the optimized geometry of the stilling basin, systematic experimental tests were carried out on a physical model in the laboratory of the BAW (Fig. 4). The tests were performed in a 2.33 m wide flume with a length of 15.00 m and a height of 0.60 m. The discharge was varied between 15 l/s ≤ Q ≤ 370 l/s. All tests were conducted with free weir overflow. The upstream water level y_u was measured by ultrasonic probes approx. 1.40 m upstream of the weir in the channel center. The measuring error of the water level probes was about ±0.1 mm. The discharge was controlled by a magnetic-inductive flowmeter (MID) and electrically adjustable valves with a measuring error of about ±0.8 l/s.

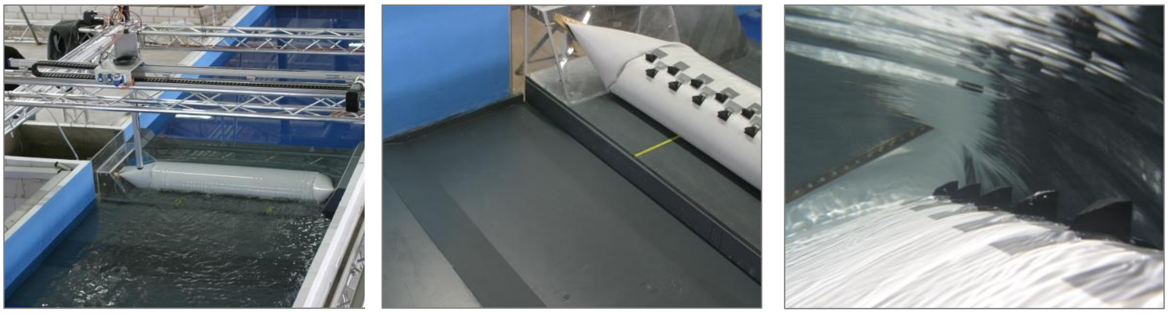

Figure 4. Physical model: rubber gate (left); weir sill with vertical apron and stilling basin with sloping end sill (Center) and row of breakers on rubber gate (right).

4. Simulation Results

4.1. Energy Dissipation Caused by Weir Sill

When the rubber gate is partly inflated and overtopped, the weir sill performs like a drop structure. This effect is typically used at stepped spillways, where a series of drops generate substantial energy losses on the spillway structure itself, thereby reducing the need for a more costly geometry of a stilling basin. In order to estimate the energy loss on the sill, simulations were carried out for eight gate heights h_d between h_d/h_u = 0.85-0.29

(Table 2), while the upstream water level y_u was kept constant and the tailwater level y_t was adjusted to achieve near critical conditions ($Fr_t = 1$) downstream of the considered stilling basin.

Table 2. Boundary conditions and results of the numerical simulations.

q [m²/s]	h_u [m]	h_d [m]	h_d/h_u [-]	c_q [-]	y_t [m]	y_t/h_u[-]
0.96	5.34	4.54	0.85	0.45	0.45	0.19
1.90	5.29	4.02	0.76	0.45	0.72	0.20
2.82	5.33	3.73	0.70	0.47	0.93	0.19
3.72	5.28	3.38	0.64	0.48	1.12	0.19
4.60	5.31	3.13	0.59	0.49	1.29	0.18
6.08	5.31	2.87	0.54	0.52	1.45	0.18
8.70	5.29	2.22	0.42	0.55	1.86	0.23
11.80	5.30	1.54	0.29	0.58	1.90	0.30

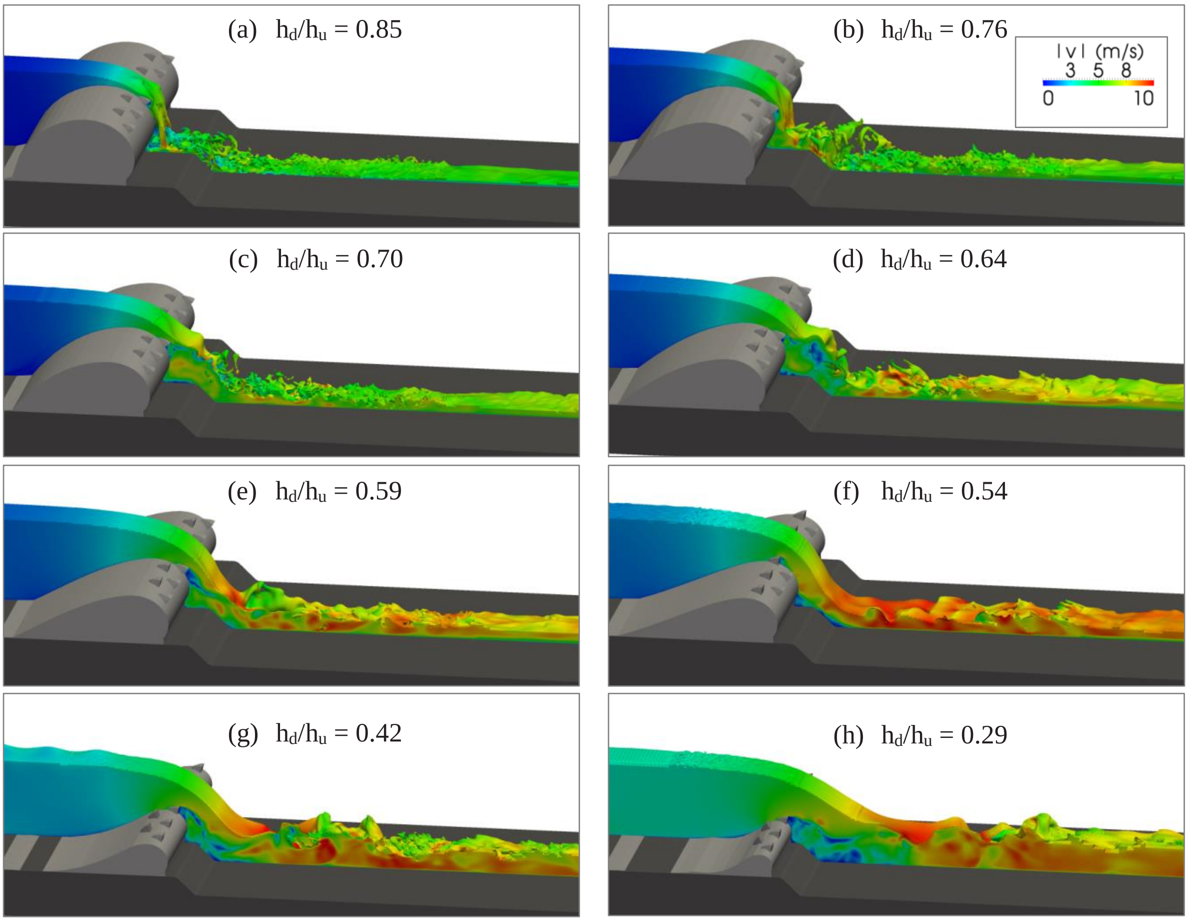

Figure 5. Simulation results for eight gate heights h_d between $h_d/h_u = 0.85$-0.29, constant upstream water level h_u and no tailwater effects ($Fr_t = 1$).

Fig. 5 shows mean velocity distributions in vertical cross sections. It can be seen that the nappe falls up to $h_d/h_u = 0.76$ completely on the weir sill. In terms of stepped spillways, this flow regime is described as nappe flow, which is defined as a series of free falling jets of water tumbling from one step to the next. Small hydraulic jumps can occur on each step, which are enhancing energy dissipation. In contrast, skimming flow is described as step tips forming a virtual-boundary above where the flow skims in a reasonably coherent stream down the spillway, although highly turbulent and aerated over much of the length of the chute (Frizell and Frizell 2015). This can be seen in Fig. 5(c) and Fig. 5(d), where the nappe partly touches the end of the weir sill. For higher discharges the nappe falls directly in the stilling basin and a recirculation zone develops under the nappe without an air chamber due to insufficient aeration, which is also called a free-falling jet with supercritical tailwater conditions.

Based on the numerical results the water depths y_1 aand corresponding Froude numbers Fr_1 were estimated and compared to the Froude numbers Fr_1 obtained by the Bernoulli equation, where the mechanical energy per unit volume of fluid moving along a streamline is assumed to be constant. For the iterative calculation the energy level $H_u = y_u + v_u/2g$ upstream of the weir was chosen. Fig. 6(a) shows a comparison of the water depths before the hydraulic jump estimated by Bernoulli equation and on basis of the numerical results. Overall, there seems to be a good agreement, but the resulting Froude numbers Fr_1 differ greatly and thus the conjugate water depth y_2. Fig. 6(b) shows the Froude numbers Fr_1 obtained by the approach of White (1943). White (1943) developed in a discussion of Moore (1943) a method to predict the energy loss at the base of an overfall. It can be seen that the Froude numbers determined by the numerical model are significantly smaller than using Bernoulli equation and are more in line with White (1943). This means, until $h_d/h_u = 0.59$, the inflow Froude number would be over-estimated, resulting in a deeper stilling basin. The Froude numbers by the use of White (1943) are for low discharges that are slightly higher. Here it should be mentioned that there remain some inaccuracies by estimating the flow depth y_1 in the numerical model. The calculation of Froude number is also quite sensitive regarding water depth variations.

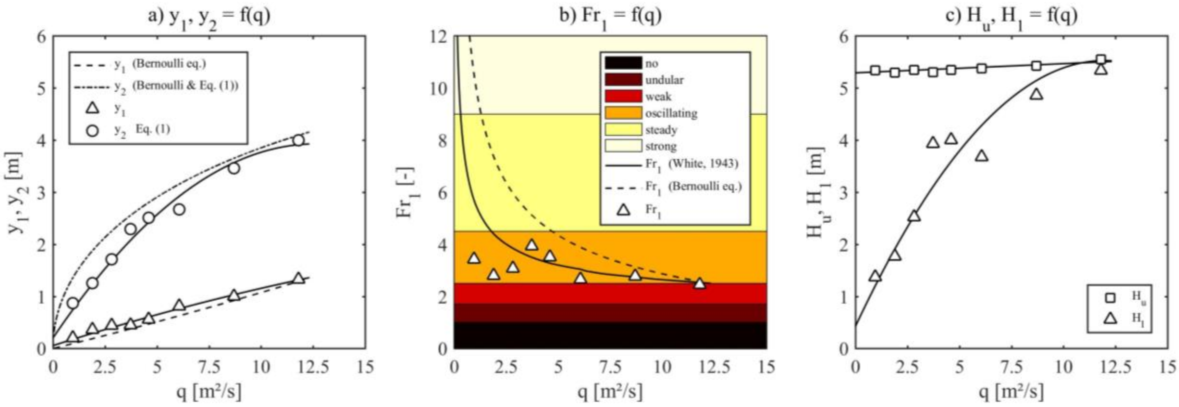

Figure 6. Comparison of (a) conjugate water depths $y_{1,2}$; (b) inflow Froude Numbers Fr_1 based on the numerical results, estimated by Bernoulli equation and by White (1943) for a drop structure and (c) energy heads H_u and H_1.

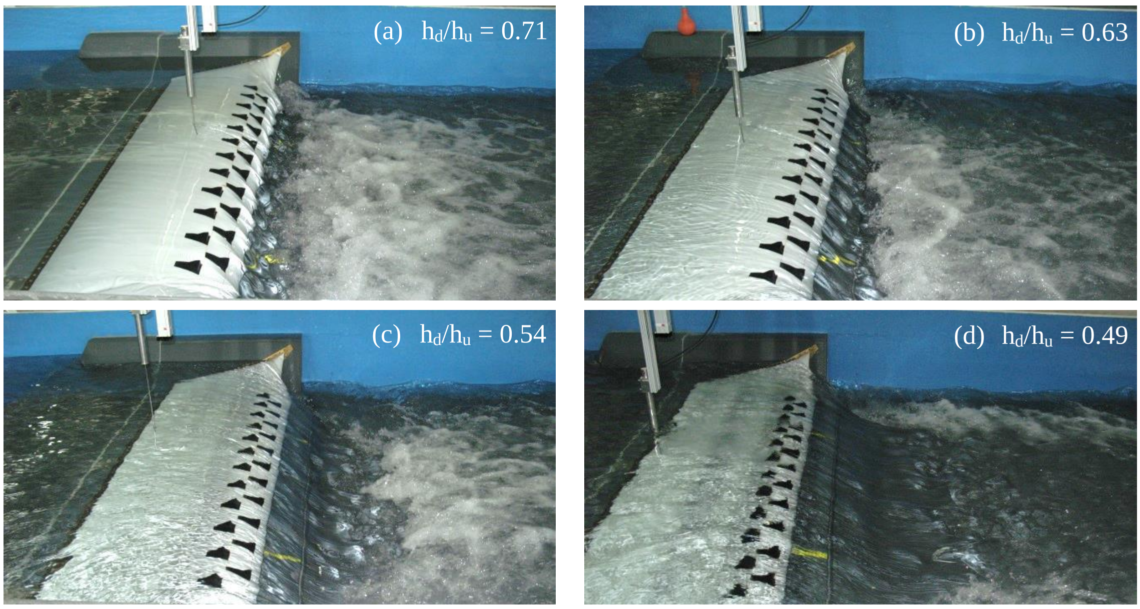

Figure 7. Development of hydraulic jump for h_d/h_u = 0.71-0.49, y_t/y_u = 0.5, y_t= 0.33 m.

Overall, the data are in fairly good agreement with the one of White (1943). The inflow Froude numbers are in the range of an oscillating jump neglecting tailwater impacts. Comparing the energy heads (Fig. 6c), it can be seen that a significant amount of dissipation takes place on the sill unless the nappe jumps directly in the stilling basin. Obviously, it would lead to significantly different water depths, resulting in a deeper stilling basin when neglecting the energy dissipation by the nappe flow.

Fig. 7 shows exemplarily the development of the hydraulic jump with increasing discharge, while the tailwater level was constant. For $h_d/h_u = 0.71$ the nappe hits the sill resulting in high energy dissipation with an accompanying air entrainment (Fig. 7a). Air entraining is reduced for skimming flow (Fig. 7b) and disappears as soon as the overfall nappe reaches the river bed (Fig. 7c). In this state, a surface roller is formed, which is pushed downstream with a further increase in discharge (Fig. 7d).

4.2. Depth and Length of Stilling Basin

Simulations were carried out following the recommendation of Blind (1987) for different submergence factors. Therefore, the tailwater level was kept constant, while the bed level was lowered resulting in a higher water depth y_t. The bed level was chosen according to Eq. (2) for a submergence factor of $\varepsilon = 1.05$ and for $\varepsilon = 1.20$. The comparison showed that although a hydraulic jump occurs, the length with supercritical conditions is for $\varepsilon = 1.05$ longer than for $\varepsilon = 1.20$. In the last case the hydraulic jump is pushed upstream and takes place immediately downstream of the weir sill requiring a shorter stilling basin. Thus, it can be concluded that in terms of safety, so the jump is not swept out of the stilling basin, a submergence factor of $\varepsilon = 1.20$ is more appropriate.

It is a challenge to estimate the hydraulic jump length, whether in field or in physical or numerical models due to the abrupt rise of water surface, surface rollers, and air entrainment. But, it is important because the end of a hydraulic jump would represent the end of the concrete floor and side walls of a conventional stilling basin. In order to identify the roller in the numerical results, the x-component of the velocity was chosen like it is illustrated in Fig. 8. The cross section without negative x-components was considered to be the end of the roller and a range was identified for the end of the hydraulic jump. In Fig. 9 the results are plotted for two different submergence factors against the empirical formulas mentioned in Table 2. The comparison shows that the length of the hydraulic jump is significantly smaller than for the empirical formulas, which can be explained by the additional energy dissipation on the weir sill but also due to different test configurations. Note that the basin length for a submergence factor of $\varepsilon = 1.20$ is significantly smaller for higher discharges and can be predicted fairly by the recommendation of Blind (1987). Based on these results a stilling basin length of $L_T = 15$ m and a depth $\delta = 1.5$ m was considered as appropriate if $Fr_t = 1$ is considered to be the most unfavorable tailwater condition.

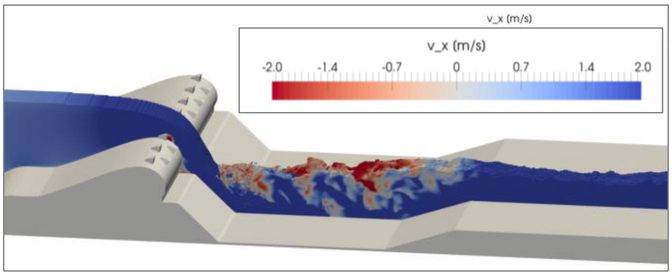

Figure 8. Direction of the horizontal velocity component v_x: (blue) in and (red) towards the main flow direction.

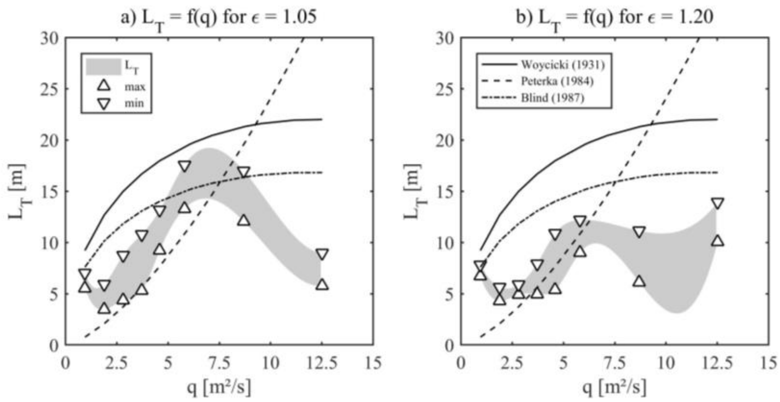

Figure 9. Length of hydraulic jump in dependence of specific discharge q in comparison to empirical formulas of Woycicki, discussed in Bollrich *et al.* (2013), Peterka (1984) and Blind (1987).

4.3. Analysis of End Sills

Generally, the height of the end sill or the depth of the stilling basin is determined by the conjugate water depth y_2 and the tailwater depth y_t. In literature a huge variety of end sills can be found, such as vertical, sloping, or dentate end sills. In this study, three types of end sills were considered based on recommendations of DIN 19661-2. Fig. 10 shows a sloping end sill and a partly sloping, partly vertical end sill both with the same height. In the last configuration the top of the end sill was one third above the bed level. This configuration was considered to be cost-effective because of less excavation works for the basin compared to the above-mentioned types. Dentate end sills were excluded because they might injure migrating fishes. Fig. 10 shows exemplarily the results for $h_d/h_u = 0.54$ for the three end sill types. It can be seen that the end sill types, which are partly vertical, direct the bottom current upward and away from the river bed resulting in a vortex behind the end sill. The stabilization of the hydraulic jump is slightly better, but scouring behind the end sill is a major concern and causes additional costs for bottom protection. Additionally, a secondary jump was feared to occur downstream of the stilling basin. Hence, the sloping end sill was considered to be an appropriate solution.

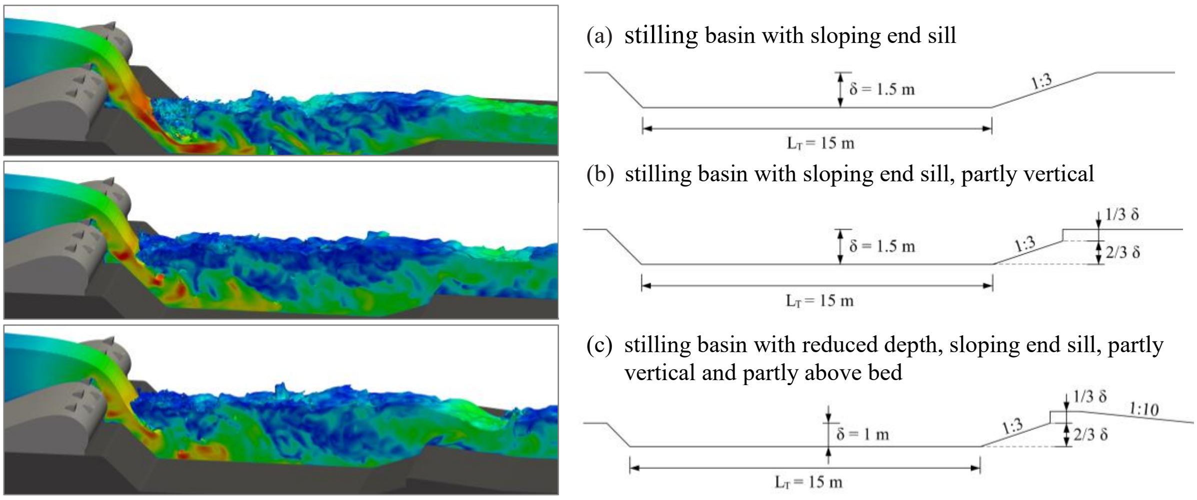

Figure 10. Simulation results for different end sill designs for $h_u = 5.31$ m, $h_d/h_u = 0.54$, $\delta = 1.50$ m, $Fr_t = 1$.

4.4. Analysis of Submerged Hydraulic Jump

In the next step, the chosen geometry for the stilling basin ($\delta = 1.5$ m, $L_T = 15.0$ m, sloped end sill) was tested under submerged conditions. Therefore, the tailwater level was increased stepwise for the critical regarded state ($h_d/h_u = 0.54$), where the overflowing nappe hits completely the floor of the stilling basin; Fig. 11 shows the performance of the stilling basin for downstream Froude numbers $1.0 > Fr_t > 0.15$ resulting in submergence factors $1.20 < \varepsilon < 2.55$. It can be seen that up to $Fr_t = 0.25$ ($\varepsilon \approx 2.00$), the hydraulic jump gets increasingly submerged without losing its hydraulic efficiency. The jet adheres to the apron surface and to the stilling basin floor. Here, the tailwater depth is smaller than the drop height. For decreasing downstream Froude numbers, the jet separates from the sill and approaches the water surface, also called plunging jet flow. For $Fr_t = 0.18$ an undular jump or undulating surface jet flow takes place and waves of large amplitudes develop and propagate downstream of the jump. It must be noted that these undulations might have an impact on the channel banks and must be taken into account for the design. According to Chanson and Montes (1995) the propagation of free-surface waves may impose also additional impact loads on downstream structures, such as locks or weirs, and might be a problem for passing vessels.

Additionally, the stilling basin was tested for variable submerged conditions, where the tailwater level increases while the discharge increases. This situation is more appropriate to natural conditions with a tailwater rating curve. Here, it was assumed that the downstream Froude number is constant $Fr_t = 0.35$. Fig. 12 shows the performance of the stilling basin. The resulting submergence factors are $1.58 < \varepsilon < 2.76$. It can be seen that the hydraulic jump stays in the stilling basin. Furthermore, it can be observed that for $h_d/h_u = 0.42$, the jet separates from the sill and approaches the water surface. For $h_d/h_u = 0.29$ an undular jump occurs.

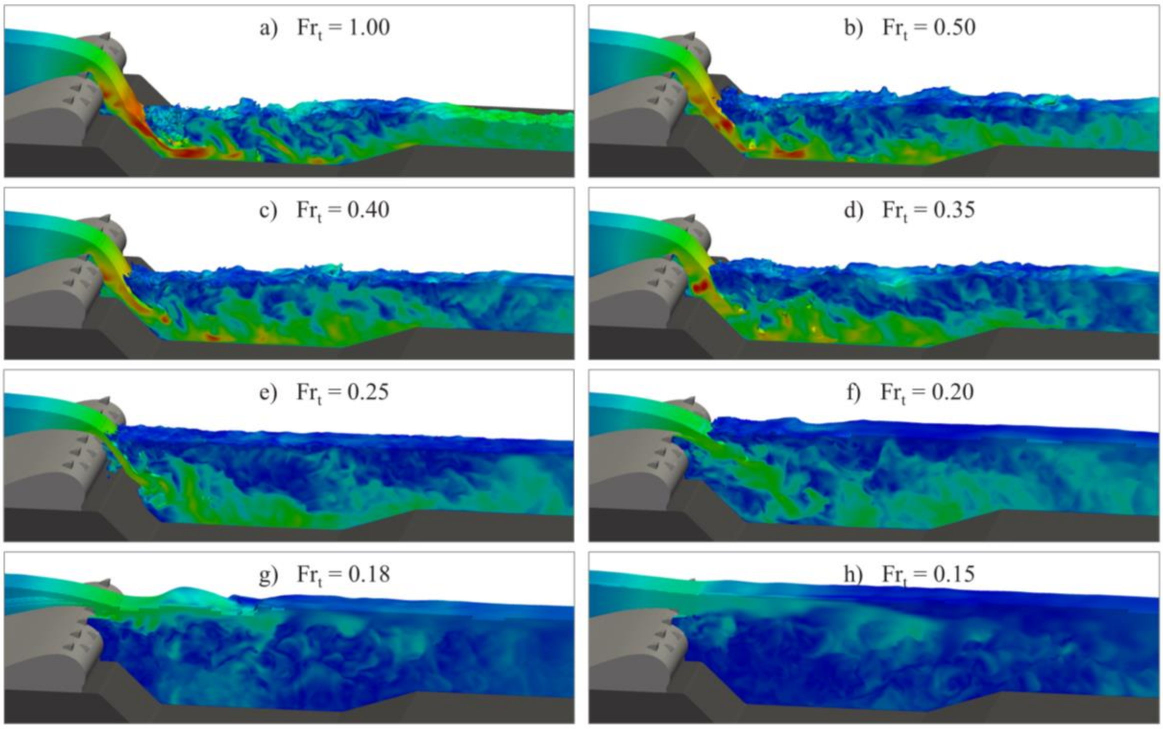

Figure 11. Effects of submergence on the performance of a submerged hydraulic jump for $h_d/h_u = 0.54$, constant upstream water level $h_u = 5.31$ m and decreasing downstream Froude Number Fr_t.

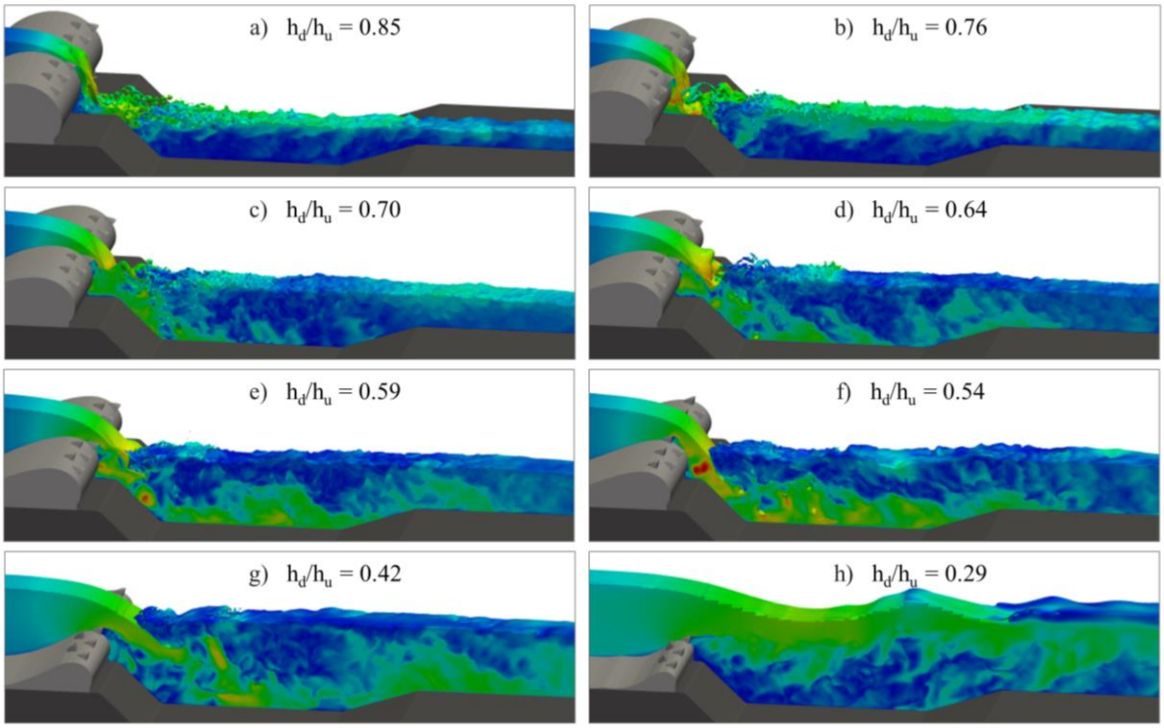

Figure 12. Development of hydraulic jump with increasing discharge $h_d/h_u = 0.85\text{-}0.29$, $Fr_t = 0.35$, $h_u= 5.31$ m.

5. Conclusions

The numerical study on the design of a stilling basin downstream of an inflatable gate showed that the energy dissipation on the weir sill has a significance influence and cannot be neglected. Up to 75 % of the energy dissipation is caused by the first step where the nappe touches the sill. This corresponds to the discharge up to approximately $h_d/h_u = 0.59$, where the inflow Froude number would be over-estimated. This is positive regarding the size of the stilling basin, which is shorter and less deep. Note that the aim of this study was to define a standard stilling basin in order to reduce the necessity for further investigations, such as with physical models. But, standardization also includes the overestimation of some states.

6. References

Bélanger, J.B. (1941). *Notes sur l'Hydraulique: (Notes on Hydraulic Engineering)*. session 1841-1842. Paris, France.

Blaisdell, F.W. (1959). *The SAF Stilling Basin: A Structure to Dissipate the Destructive Energy in High-velocity Flow from Spillways*. Agricultural Research Service.

Blind, H. (1987). *Wasserbauten aus Beton*. Handbuch für Beton-, Stahlbeton- und Spannbetonbau. W. Ernst, Berlin.

Bollrich, G., Martin, H., and Preißler, G. (2013). *Technische Hydromechanik*. Bauwesen : Wissen. 7. Aufl. Verl. für Bauwesen, Berlin.

Chanson, H. (2009). "Current knowledge in hydraulic jumps and related phenomena. A survey of experimental results." *European Journal of Mechanics - B/Fluids,* 28(2), 191–210.

Chanson, H., and Montes, J.S. (1995). "Characteristics of Undular Hydraulic Jumps: Experimental Apparatus and Flow Patterns." *J. Hydraul. Eng.,* 121(2), 129–144.

Chow, V.T. (1959). *Open-Channel Hydraulics*. McGraw-Hill Book Company.

DIN 19661-2. (2000). *Richtlinien für Wasserbauwerke - Sohlenbauwerke - Teil 2: Abstürze, Absturztreppen, Sohlenrampen, Sohlengleiten, Stützschwellen, Grundschwellen, Sohlenschwellen* (Ausgabe 2000-09). Beuth Verlag GmbH.

Frizell, W.K., and Frizell, K.H. (2015). Guidelines for Hydraulic Design of Stepped Spillways: A Water Resources Technical Publication. Hydraulic Laboratory Report HL-2015-06.

Gebhardt, M., Pfrommer, U., Belzner, F., and Eisenhauer, N. (2012). "Backwater effects of Jambor weir sill." *Journal of Hydraulic Research*, 50(3), 344–349.

George, R.L. (1978). Low Froude Number Stilling Basin Design. *Report No. REC-ERC-78-8*. Engineering and Research Center.

JIID. (1986). *Land Consolidation: Engineering Manual for Irrigation and Drainage*. Japanese Institute of Irrigation and Drainage (JIID).

Marmulla, G., ed. (2001). *Dams, fish and fisheries: Opportunities, challenges and conflict resolution*. FAO fisheries technical paper, 419. FAO, Rome, eng.

Moore, W.L. (1943). Energy loss at the base of a free fall. *Transactions of the American Society of Civil Engineers,* 1(108), 1343–1360.

Peterka, A.J. (1984). Engineering Monograph No. 25, “Hydraulic Design of Stilling Basins and Energy Dissipators.” *Engineering Monograph 25*. Bureau of Reclamation, Denver, Colorado.

PIANC, ed. (2018). *Inflatable Structures in Hydraulic Engineering: InCom Working Group 166*. in press.

Rajaratnam, N. (1965). Submerged Hydraulic Jump. *Journal of the Hydraulics Division,* (4), 71–96.

Rouse, H. (1967). *Engineering hydraulics: Proceedings of the 4. Hydraulics Conference, Iowa Institute of Hydraulic Research, June 12-15, 1949*. 6. print. Wiley, New York [u.a.].

Rusche, H. (2002). Computational Fluid Dynamics of Dispersed Two-Phase Flows at High Phase Fractions. *Dissertation*. Imperial College, London.

Singh, V.P., and Hager, W.H. (1992). *Energy Dissipators and Hydraulic Jump,* 8. Springer Netherlands, Dordrecht.

Thorenz, C., and Strybny, J. (2012). "On the numerical modelling of filling-emptying systems for locks." In *Proceedings of 10th International Conference on Hydroinformatics: HIC 2012; understanding changing climate and environment and finding solutions; Hamburg, Germany, July 14-18, 2012*. 1 CD-ROM. R. Hinkelmann, Y. Liong, D. Savic, M.H. Nasermoaddeli, K.F. Daemrich, P. Fröhler, D. Jacob, eds. TuTech Innovation, Hamburg.

White, M.P. (1943). "Discussion of Moore, W.L. Energy loss at the base of free overfalls." *Transactions of the American Society of Civil Engineers,* 1(108), 1361–1364.